The American Journal of Pathology, Vol. 170, No. 2, February 2007

DOI: 10.2353/ajpath.2007.060761

Vascular Biology, Atherosclerosis and Endothelium Biology

Tumor-Induced Sentinel Lymph Node Lymphangiogenesis and Increased Lymph Flow Precede Melanoma Metastasis

Maria I. Harrell,* Brian M. Iritani,† and Alanna Ruddell*

From the Division of Basic Sciences, Fred Hutchinson Cancer Research Center, Seattle; and the Department of Comparative Medicine,† University of Washington, Seattle, Washington*

Lymphangiogenesis is associated with human and murine cancer metastasis, suggesting that lymphatic vessels are important for tumor dissemination. Lymphatic vessel alterations were examined using B16-F10 melanoma cells implanted in syngeneic C57Bl/6 mice, which form tumors metastasizing to draining lymph nodes and subsequently to the lungs. Footpad tumors showed no lymphatic or blood vessel growth; however, the tumor-draining popliteal lymph node featured greatly increased lymphatic sinuses. Lymph node lymphangiogenesis began before melanoma cells reached draining lymph nodes, indicating that primary tumors induce these alterations at a distance. Lymph flow imaging revealed that nanoparticle transit was greatly increased through tumor-draining relative to nondraining lymph nodes. Lymph node lymphatic sinuses and lymph flow were increased in mice implanted with unmarked or with foreign antigen-expressing melanomas, indicating that these effects are not due to foreign antigen expression. However, tumor-derived immune signaling could promote lymph node alterations, as macrophages infiltrated footpad tumors, whereas lymphocytes accumulated in tumor-draining lymph nodes. B lymphocytes are required for lymphangiogenesis and increased lymph flow through tumor-draining lymph nodes, as these alterations were not observed in mice deficient for B cells. Lymph node lymphangiogenesis and increased lymph flow through tumor-draining lymph nodes may actively promote metastasis via the lymphatics. ***(Am J Pathol 2007, 170:774–786; DOI: 10.2353/ajpath.2007.060761)***

The contribution of the lymphatic system to tumor metastasis is being increasingly appreciated through studies of murine as well as human cancers.[1] The discovery of the vascular endothelial growth factors VEGF-C and VEGF-D, which activate lymphatic vessel growth by stimulating VEGF receptor (VEGFR)-3 expressed on lymphatic endothelium, allowed examination of the role of lymphangiogenesis in tumor dissemination.[2,3] In mice, VEGF-C or VEGF-D overexpression promotes tumor lymphangiogenesis and lymph node (LN) metastasis,[4–6] whereas inhibition of VEGFR-3 signaling blocks lymphatic vessel growth and tumor dissemination.[7,8] In human cancers, increased VEGF-C or VEGF-D expression is often associated with metastasis or poor prognosis.[2,3] Moreover, identification of tumor cells in tumor-draining sentinel LNs is increasingly used to diagnose metastatic cancers, including melanoma and breast cancer.[9,10] These findings indicate that the lymphatic system is involved in tumor dissemination to secondary organs, presumably by lymphatic delivery to the lymph nodes and to the systemic circulation via the thoracic duct. Abnormal blood vessel growth in tumors can alternatively promote tumor dissemination via the bloodstream, so that the lymphatic or the vascular systems can mediate metastasis depending on the particular type of cancer examined.[1]

Although the contribution of lymphatic vessels to tumor metastasis has been experimentally demonstrated, little is known yet about the mechanisms involved in tumor dissemination via the lymphatics. High tumor interstitial fluid pressure is thought to promote tumor cell entry into lymphatic vessels that have lower fluid pressure.[11,12] Intratumoral lymphatic vessel growth often correlates with metastasis of human melanoma, breast, or head and neck cancers,[13–15] where tumor cells can be observed within lymphatic vessels, suggesting that lymphatic vessel growth is important for tumor spread. However, stud-

Supported by National Institutes of Health (NIH) grant CA68328, a University of Washington/Fred Hutchinson Cancer Research Center Consortium Pilot grant, a Fred Hutchinson Cancer Research Center New Technology Development grant (to A.R.), and NIH grant AI053568 (to B.M.I.).

Accepted for publication October 31, 2006.

Address reprint requests to Alanna Ruddell, Fred Hutchinson Cancer Research Center, 1100 Fairview Ave. N., MS-C2-023, P.O. Box 19024, Seattle, WA 98109. E-mail: aruddell@fhcrc.org.

ies of murine and human tumors indicated that intratumoral lymphatics are often nonfunctional,[12] whereas expansion of peritumoral lymphatic vessels could instead mediate metastasis.[16] Moreover, a recent study demonstrated that inhibition of lymphangiogenesis does not block metastasis to tumor-draining LNs in mice.[17] Hence, much remains to be learned about how tumor cells enter and travel through lymphatic vessels and lymph nodes during metastasis to secondary organs.

Diagnosis of cancer metastasis frequently involves examining tumor-draining sentinel LNs for cancer cells. However, an active role of sentinel LNs in tumor dissemination via the lymphatics has not been considered until recently. We discovered extensive lymphangiogenesis in LNs from Eμ-*c-myc* transgenic mice developing lymphomas[18] even before the development of lymphomas, which could contribute to lymphoma dissemination. In this model, Myc-expressing immature B cells accumulate in LN before progressing to form a highly metastatic lymphoma.[19] LNs of Eμ-*c-myc* mice exhibit active lymphatic sinus growth at early stages of lymphoma formation, whereas lymphatic vessels in other organs are unaffected.[18] Lymphangiogenesis within LNs from Eμ-*c-myc* mice is accompanied by a 23-fold increase in lymph flow through LNs, as determined by a footpad dye injection assay. These findings led us to propose that LN lymphangiogenesis and increased lymph flow could actively promote dissemination of lymphomas to secondary organs.

Our discovery of LN lymphangiogenesis in mice developing metastatic B cell lymphomas suggested that the LN could also be involved in lymphatic dissemination of solid tumors. In this study, we used the B16-F10 metastatic melanoma model to examine whether alterations of tumor or LN lymphatic vessels arise in mice developing metastatic solid tumors. The B16-F10 melanoma cell line was derived from a spontaneous melanoma arising in a C57Bl/6 mouse.[20] Footpad injection of these cells produces metastatic melanoma detected in the tumor-draining LN and subsequently in the lungs.[21] In this study, we identified extensive LN lymphangiogenesis and increased lymph flow through LNs draining B16 melanomas, which could promote dissemination of these tumors via the lymphatics.

Materials and Methods

Mouse Tumor Models

B16-F10 murine melanoma cells (American Type Culture Collection, Manassas, VA) were tested for mycoplasma or virus contamination before injection into mice (Research Animal Diagnostic Laboratory, University of Missouri, Columbia, MO). In some experiments, Anjou 293 packaging cells[22] were transiently transfected with the LXCG plasmid, a defective murine retroviral vector[23] encoding enhanced green fluorescent protein (GPF) (Clontech Laboratories, Inc., Mountain View, CA) downstream of the human cytomegalovirus immediate early promoter (generously provided by Dr. John Rasko, University of Sydney, Sydney, Australia). Viral supernatants were collected and incubated with B16 cells in 8 μg/ml Polybrene (Sigma-Aldrich, St. Louis, MO) for 2 days. Transduced cells were flow sorted for GFP positivity.

Four- to 5-week-old C57BL/6J wild-type, homozygous C57BL/6J-Tyr$^{C\text{-}2J}$/J albino (carrying a spontaneous mutation in the tyrosinase gene), or homozygous μMT C57Bl/6 mice deficient for B lymphocytes were obtained from Jackson Laboratories (Bar Harbor, ME) and maintained in sterile microisolator rooms. Mice were injected in one hind footpad with 200,000 GFP-expressing or unmarked B16-F10 cells in a 50-μl volume of Hanks' buffered saline solution,[21] whereas the other footpad was injected with saline solution alone. After 18 to 22 days, mice were imaged under anesthesia for 30 minutes (see below) and euthanized with CO_2, and tissues were dissected. Experimental methods involving animals were approved by the Fred Hutchinson Cancer Research Center Animal Care and Use Committee.

Immunostaining and Flow Cytometry

Footpads or LN were serially sectioned to analyze the entire tissue. Eight-μm cryosections were fixed in acetone for 10 minutes, dried for 15 minutes, and formalin-fixed for 10 minutes, followed by 30 minutes of treatment with 0.3% hydrogen peroxide in methanol. Sections were immunostained with the following antibodies: MECA-32 (BD Biosciences, Bedford, MA), 10.1.1,[24] 8.1.1,[24,25] CD31 (BD Biosciences), or LYVE-1 (Upstate, Temecula, CA). Immunostaining was detected using horseradish peroxidase-labeled secondary antibodies with Vector VIP followed by methyl green counterstaining (Vector Laboratories, Burlingame, CA). Lymphatic vessel area was measured in 616 $\times$ 484-μm fields of 100$\times$ magnification images of 10.1.1 antibody-stained LN sections, using the NIH ImageJ program (National Institutes of Health, Bethesda, MD). Blood vessel area or density was similarly measured in LN sections immunostained with MECA-32 antibody. Individual lymphatic or blood vessels in the footpad were visually hand-counted by direct examination of microscope fields at $\times$100 magnification. Statistical analysis was performed by the two-tailed Student's *t*-test.

Immunofluorescent staining with mitotic phosphohistone H3 (Upstate), 10.1.1, GFP (Molecular Probes, Eugene, OR), F4/80 (eBioscience, San Diego, CA), or control antibodies used acetone and formalin fixation and detection with fluorescein isothiocyanate (FITC)- or Alexa-labeled secondary antibodies (Molecular Probes) followed by mounting in DAPI-containing media (Vectashield; Vector Laboratories). Fixed sections were also directly immunostained with FITC-labeled MI/70 Mac-1 (BD Biosciences), rat IgG2b (BD Biosciences), or B220 antibodies (Caltag, Carlsbad, CA) after blocking with CD16/CD32 antibody to Fc receptor (Fc Block, BD Biosciences).

The lymphocyte composition of LNs was determined by LN dissociation between frosted glass slides, nylon filtration, cell counting in a hemocytometer, and immuno-

staining with FITC-CD3 and PE-B220 (Caltag) followed by propidium iodide staining and flow cytometry.

Optical Imaging

Real-time fluorescence images were obtained using a Xenogen IVIS Imaging System 100 equipped with a Cy5.5 filter set (Xenogen, Alameda, CA). Identical illumination settings (lamp voltage, filters) were used for all images, and fluorescence emission was normalized to fluorescent efficiency, where the value of each pixel in an efficiency image represents the fractional ratio of fluorescent emitted photons per incident excitation photon.[26]

Mice were anesthetized with 2 to 3% isoflurane, and were positioned supine in the Xenogen IVIS, with legs taped to expose the popliteal fossa. The dorsal toe of each hindfoot was then injected with 25 μl of Qtracker 705 nontargeted quantum dots (Qdot Corporation, Hayward, CA) or with 25 μl of Cy5.5-labeled magnetic nanoparticles (Nanocs, Inc., New York, NY), both diluted 1:1 in 0.3% Evans blue (Sigma-Aldrich) in saline. For determining lymph flow, total fluorescent efficiency of the popliteal LN area of the right and left leg of the animal were calculated over regions of interest using Living Image software (Xenogen) integrated with Igor (Wavemetrics, Lake Oswego, OR). Preinjection images were used to subtract background autofluorescence in the region of interest. Statistical analysis was performed with a two-tailed Student's paired *t*-test.

Results

Lymphatic and Blood Vessels Are Normal in B16 Footpad Tumors

The B16 melanoma cell line reliably undergoes metastasis to the tumor-draining popliteal LN and subsequently to the lungs within a few months after implantation in the footpad of syngeneic C57Bl/6 mice.[21] The lymphatics of the foot drain directly through the popliteal LN,[27] which is advantageous for analysis of tumor spread through the draining LN. We used this model to characterize lymphatic and blood vessels in the primary tumor and draining popliteal LN as a first step to examine the involvement of the lymphatic system in dissemination of these tumors. Four-week-old albino C57Bl/6 mice were injected in one rear footpad with B16 cells, whereas the other rear footpad was injected with saline as an internal control. The melanoma cells were infected with a GFP-expressing retroviral vector to monitor tumor cell metastasis. Footpad tumors and LN were analyzed 18 to 22 days after tumor implantation, when tumors reached a 3- to 6-mm diameter.

Serial sections of the resulting melanomas were analyzed by immunostaining with the 10.1.1 antibody, which specifically recognizes murine lymphatic endothelium.[18,24] The growing melanomas did not obviously alter the lymphatic vessels of the footpad. Lymphatic vessels are sparse in the control leg footpad and are also rarely observed within the footpad tumor (Figure 1A, arrows).

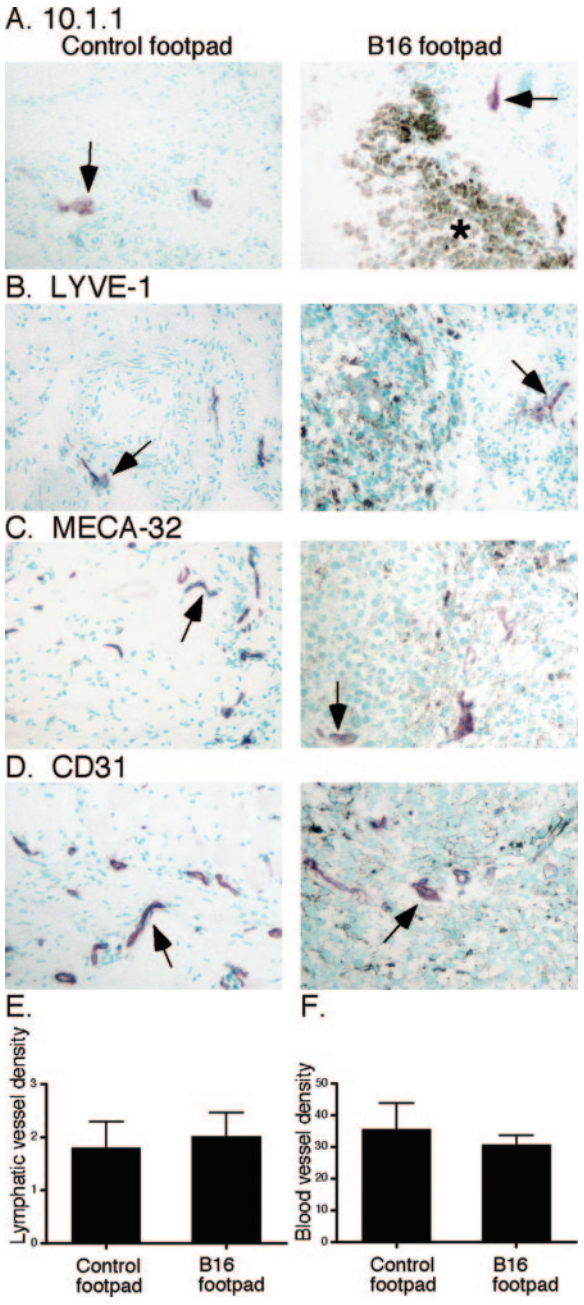

Figure 1. Normal representation of lymphatics and blood vessels in footpad melanomas in albino mice. **A:** Control footpad or B16 footpad tumor immunostained with 10.1.1 lymphatic endothelial antibody both show sparse purple-stained lymphatic vessels (**arrows**) with methyl green counterstaining. The black melanin pigment identifies the B16 tumor (right panel, **asterisk**). **B:** LYVE-1 immunostaining also identifies sparse lymphatic vessels (**arrows**) in control (left panel) or B16 footpads (right panel). **C:** Blood vessels immunostained with MECA-32 antibody (**arrows**) are similar in control footpads (left panel) and in footpad tumors (right panel). **D:** CD31 immunostaining also shows similar blood vessels in control and B16 footpads. All panels are shown at ×100 magnification. **E:** Image quantification demonstrates similar lymphatic vessel density in seven control and 10 B16 tumor-bearing footpads. **F:** Image quantification confirms similar blood vessel density in seven control and eight tumor-bearing footpads. Standard errors are shown.

Previous studies suggested that abnormal lymphatic vessels in the tumor periphery could mediate lymphatic metastasis.[16] However, we did not observe any increase in the number or size of occasional peritumoral lymphatic

vessels. Immunostaining with the LYVE-1 antibody, which also recognizes lymphatic endothelium[28] confirmed that lymphatic vessels are sparse in control footpads or in tumors (Figure 1B). These visual observations were confirmed by counting vessel density in regions spanning footpad tumors or in corresponding regions of the control leg footpad. Lymphatic density was similar in tumors and in control footpads (Figure 1E). These findings indicate that B16 melanoma growth within the footpad is not accompanied by intratumoral or peritumoral lymphatic vessel growth.

Blood vessels in or around B16 footpad tumors were also unaffected by tumor growth, as shown by immunostaining with the vascular endothelial-specific MECA-32 antibody[29] (Figure 1C, arrows). This finding was confirmed by immunostaining for CD31 (Figure 1D). Quantitation of MECA-32-positive vessels showed similar blood vessel density in tumors and in control footpads (Figure 1F). These findings indicate that B16 tumors do not obviously alter the vascular supply at early stages of tumor growth.

Lymph Node Lymphangiogenesis Is an Early Response to Tumor Growth

Our finding that footpad melanomas fail to induce lymphatic or blood vessel growth suggested that some other mechanism promotes B16 tumor dissemination. The popliteal LN draining the footpad melanoma was examined to determine whether vessels in this lymphatic organ are altered by tumor growth. 10.1.1 immunostaining of the control leg popliteal LN showed sparse lymphatic sinuses restricted to the cortex (Figure 2A). However, the popliteal LN from the tumor-draining leg showed greatly increased and enlarged lymphatic sinuses distributed throughout the cortex and medulla (Figure 2, B and C). Lymphangiogenesis was consistently observed in the tumor-draining LNs from 10 mice whether the tumor was implanted in the left or right foot (data not shown). The LYVE-1 antibody, which also recognizes lymphatic endothelium,[28] shows the expanded lymphatic sinuses (Figure 2H) in a pattern similar to that obtained with the 10.1.1 antibody (Figure 2, B and C). The 8.1.1 antibody to podoplanin expressed on lymphatic endothelium[30] also recognized these lymphatic sinuses (data not shown), confirming that lymphatic endothelium is increased within these LNs. These findings indicate that the tumor somehow promotes expansion of lymphatic sinuses in the draining LN.

Quantification of the area occupied by 10.1.1-positive lymphatic vessels in LNs by NIH ImageJ measurement of microscope images demonstrated a ninefold increase in lymphatic vessel area in the tumor-draining LNs relative to the control LNs (Figure 3A). These data confirm that lymphatic sinus expansion is consistently induced in the tumor-draining LN within 3 weeks after tumor implantation in the footpad. The effects of the melanomas on lymphatic vessels are restricted to the tumor-draining LNs, as control leg popliteal LNs from tumor-bearing mice showed the same sparse pattern of lymphatic sinuses (Figure 2A) as popliteal LNs from normal littermates (data not shown). Moreover, the nondraining mesenteric LN of tumor-bearing or control mice showed normal lymphatic sinuses (data not shown).

The expansion of lymphatic sinuses in the tumor-draining LN could result from the proliferation of lymphatic endothelial cells. We tested whether lymphatic endothelial cell proliferation is involved by immunostaining LN with anti-phosphohistone H3 antibody that recognizes a phosphorylated serine 10 residue specific for mitotic cells.[31] Punctate phosphohistone staining of mitotic nuclei was often detected in 10.1.1-positive lymphatic endothelial cells in tumor-draining LNs (Figure 2G, arrows), whereas phosphohistone staining was rarely observed in control LNs (data not shown). Actively dividing cell populations show 1 to 2% positivity for mitotic phosphohistone H3,[32] so that our frequent detection of mitotic lymphatic endothelium indicates that proliferation contributes at least in part to the expansion of lymphatic sinuses in tumor-draining LN.

Lymph Node Lymphangiogenesis Precedes Tumor Metastasis

To determine whether the LN alterations are associated with invasion by melanoma cells, we analyzed tumor-draining LNs for the presence of melanoma cells. Sections throughout the entire LN were either directly examined for immunofluorescent GFP cells, were stained with GFP antibodies, or examined by light microscopy for the black-pigmented melanoma cells. The lungs of these animals did not yet contain metastases, in agreement with previous studies showing that lung metastases are not visible until several months after implantation.[21] At 18 to 22 days after implant, only two of 10 LNs contained pigmented metastases that were GFP-positive (Figure 2I, arrow), whereas one LN contained a small cluster of GFP-positive cells (data not shown). The other seven nonmetastatic tumor-draining LNs showed no sign of melanin- or GFP-positive (Figure 2J) cells. The extent of lymphangiogenesis in LNs containing metastases (Figure 2B) was similar to that observed in LNs that did not yet contain melanoma cells (Figure 2C). These findings suggest that tumors in the foot act at a distance to induce lymphangiogenesis within the popliteal LN before melanoma cells are detectible within the LN. On the other hand, a small number of undetected tumor cells within the LN could potentially provoke this strong response.

We tested whether the tumor-draining LN also undergo angiogenesis in response to tumor-derived signals. MECA-32 immunostaining identified capillaries and high endothelial venules throughout the cortex and medulla of the control leg popliteal LN (Figure 2D). The pattern of MECA-32 antibody immunostaining was similar in the tumor-draining popliteal LNs with (Figure 2E) or without (Figure 2F) metastasis. Quantitation of blood vessel area (Figure 3B) or density (Figure 3C) from microscope images using the NIH ImageJ program confirmed that there was no significant blood vessel

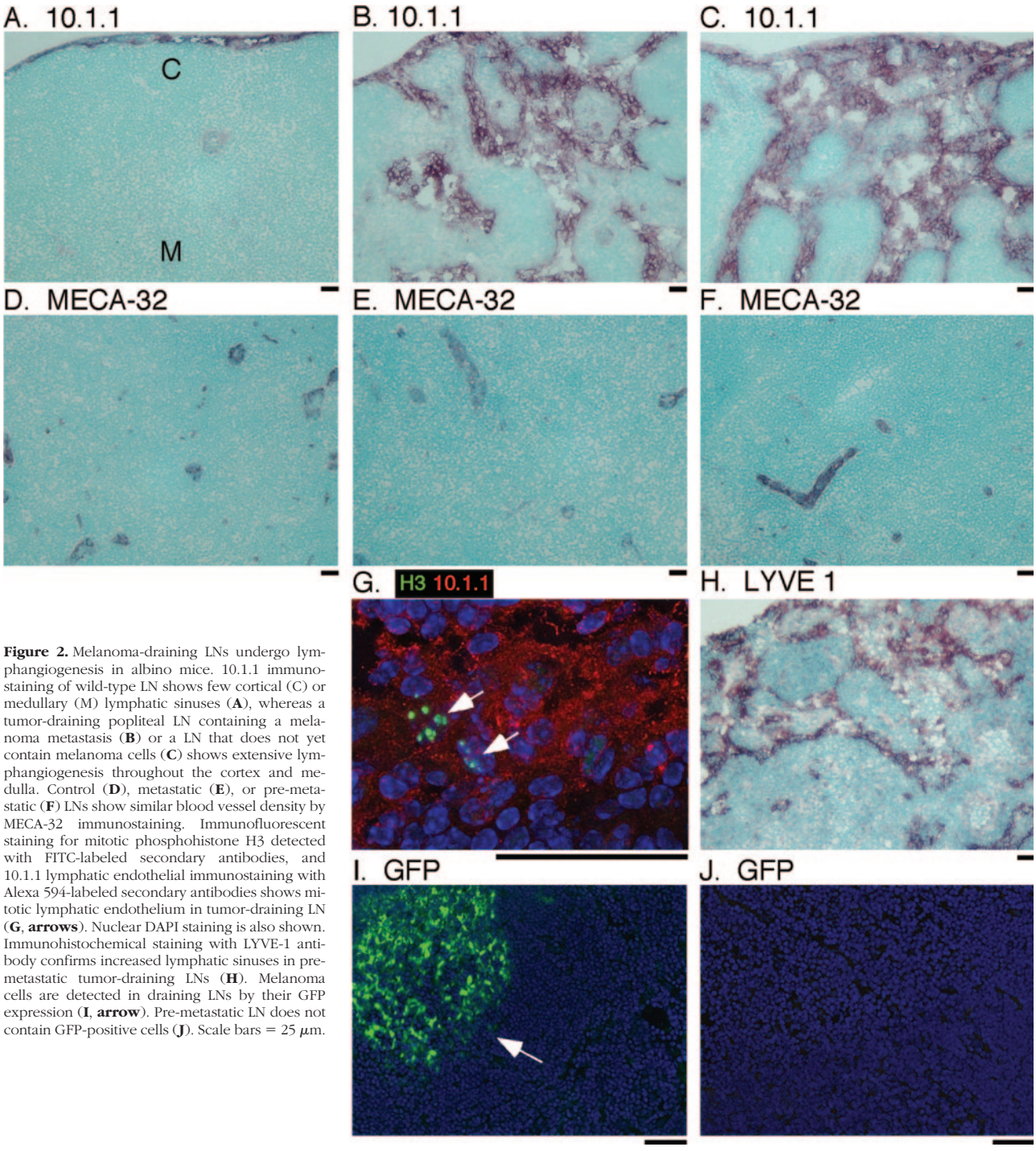

Figure 2. Melanoma-draining LNs undergo lymphangiogenesis in albino mice. 10.1.1 immunostaining of wild-type LN shows few cortical (C) or medullary (M) lymphatic sinuses (**A**), whereas a tumor-draining popliteal LN containing a melanoma metastasis (**B**) or a LN that does not yet contain melanoma cells (**C**) shows extensive lymphangiogenesis throughout the cortex and medulla. Control (**D**), metastatic (**E**), or pre-metastatic (**F**) LNs show similar blood vessel density by MECA-32 immunostaining. Immunofluorescent staining for mitotic phosphohistone H3 detected with FITC-labeled secondary antibodies, and 10.1.1 lymphatic endothelial immunostaining with Alexa 594-labeled secondary antibodies shows mitotic lymphatic endothelium in tumor-draining LN (**G**, **arrows**). Nuclear DAPI staining is also shown. Immunohistochemical staining with LYVE-1 antibody confirms increased lymphatic sinuses in pre-metastatic tumor-draining LNs (**H**). Melanoma cells are detected in draining LNs by their GFP expression (**I**, **arrow**). Pre-metastatic LN does not contain GFP-positive cells (**J**). Scale bars = 25 μm.

growth in the tumor-draining popliteal LN. These findings indicate that B16 tumors activate lymphangiogenesis within the draining LN without inducing blood vessel growth.

LN Lymphangiogenesis Is Accompanied by Increased Lymph Flow

We previously found that LN lymphangiogenesis in Eμ-*c-myc* mice is accompanied by a 23-fold increase in lymph flow as measured by incorporation of TRITC dextran into draining popliteal and iliac LNs after footpad injection.[18] Here, we developed a real-time imaging assay to measure lymph flow in B16 tumor-bearing mice to determine whether the lymphangiogenesis we identified in melanoma-draining LN is also associated with a functional increase in lymph transit. In this assay, near-infrared fluorescent nanoparticles are injected into the rear toes, followed by imaging of lymph flow in the Xenogen IVIS imaging system. Quantum

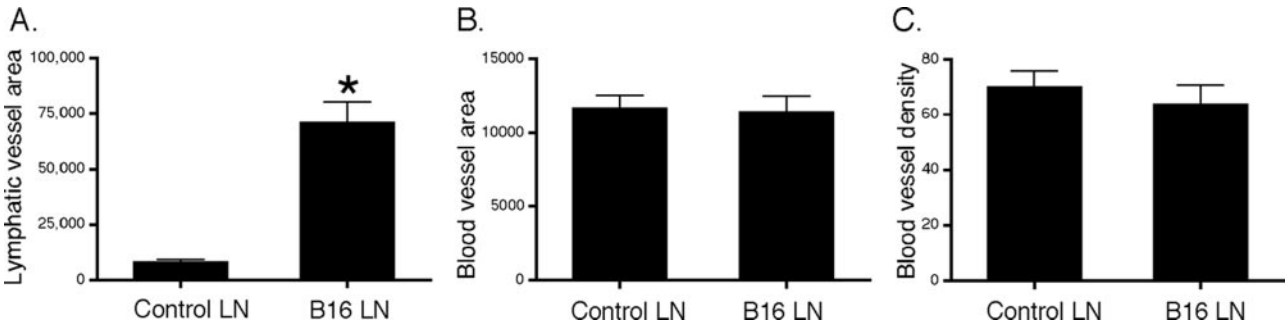

Figure 3. Lymphangiogenesis in the tumor-draining LN is not associated with angiogenesis. Measurement of 10.1.1-positive lymphatic vessel area in seven control and seven tumor-draining leg popliteal LNs shows a ninefold increase in lymphatic vessels (**A**). This increase is statistically significant by *t*-test ($N = 34$, $^*P < 0.0001$). In contrast, MECA 32-positive blood vessel area (**B**) and density (**C**) are similar in control and tumor-draining leg popliteal LNs ($N = 36$). Standard errors are shown.

dots of 52-nm diameter and Cy5.5-labeled nanoparticles of 30-nm diameter were tested. Both of these nanoparticles are of optimal size to be transported into the lymph but not into the blood stream.[33] Mice were injected in the dorsal toe located several millimeters away from the ventral footpad tumor. Immunostaining analysis showed sparse lymphatic vessels in the dorsal toe, which were similar in the tumor-bearing and control legs (data not shown).

Mice bearing left footpad melanomas were imaged from 2 to 30 minutes after injection of quantum dots into both rear toes. Quantum dots were detected within 2 minutes in the tumor-draining popliteal LN (Figure 4A, P), whereas they were not detected in the control leg LN. This increased uptake into the tumor-draining popliteal LN persisted for over 30 minutes, whereas the control LN slowly developed a detectible signal by 30 minutes after injection. All eight mice imaged with quantum dots or with Cy5.5 nanoparticles showed much more lymph flow through the tumor-draining popliteal LN. As a control, normal littermates were injected with nanoparticles in both feet. Nanoparticles were not visible in either popliteal LN of normal littermates until 30 minutes after injection (Figure 4B), confirming that increased lymph flow is restricted to tumor-draining LNs.

Lymph from the foot primarily drains through the popliteal LN and then to the internal iliac LN, whereas some lymph also drains through the inguinal and axillary LNs.[27] Quantum dots were also detected within 2 minutes in the inguinal (Figure 4A, I) and axillary LN (Figure 4A, A) draining the tumor, and these signals increased over 30 minutes of imaging. *Ex vivo* imaging of these LNs after euthanasia and dissection confirmed that they contained quantum dots (data not shown). These findings indicate that tumors can affect lymph flow for some distance through the draining lymphatic system. However, in most of the mice Xenogen detection of nanoparticles was limited to the popliteal LN. We were also unable to detect lymph flow through the tumor-draining iliac LN. This is probably due to their internal location in the peritoneum, where fluorescence is quenched. However, Evans blue dye co-injected with the nanoparticles preferentially accumulated in the iliac LN draining the tumor-bearing leg in mice autopsied within minutes after dye injection (data not shown), indicating that lymph flow through visceral tumor-draining LNs is also increased.

Lymph flow was quantitated in tumor-bearing and control mice injected with quantum dots or Cy5.5 nanoparticles by measuring the fluorescent signal (fluorescent efficiency) in a region of interest over each popliteal LN. On average, high levels of nanoparticles were detected in the tumor-draining popliteal LN within less than 2 minutes after injection, and these high levels persisted for 30 minutes (Figure 4C). In the control leg, popliteal LN signal increased at a slower rate (Figure 4D). Lymph flow was compared between the popliteal LN of the tumor-draining and control legs of individual mice to more accurately assess the difference in lymph flow rate. Lymph flow through the tumor-draining LN was 21-fold higher within 2 minutes, decreasing to twofold over normal by 30 minutes after injection (Figure 4E). Normal littermates showed no difference in lymph flow in either leg at any time point (Figure 4F). These data demonstrate that lymph flow is specifically increased through tumor-draining LNs.

Tumor Lymphangiogenesis Is Not Due to Melanin or GFP Antigen-Induced Immune Response

The melanoma cells used for these studies were engineered to express exogenous GFP to assist in monitoring for tumor cell metastasis to LNs. Moreover, these tumor transplant studies were performed using albino C57Bl/6 mice, which do not produce melanin, for optimal fluorescent imaging of lymph flow.[26] Hence we investigated whether the LN alterations we identified could involve an immune response to the foreign GFP or melanin antigens in albino mice by transplanting unmodified melanoma cells to establish tumors in black C57Bl/6 (melanin-positive) mice. Black C57Bl/6 mice developed 3- to 6-mm tumors with similar kinetics as albino (melanin-negative) C57Bl/6 mice bearing GFP-positive melanomas and showed a similar incidence of detectible LN metastases in 2 of 10 mice. The tumor-bearing footpads of the black mice showed no obvious growth of lymphatic or blood vessels as determined by immunostaining (data not shown). In contrast, the tumor-draining popliteal LN of

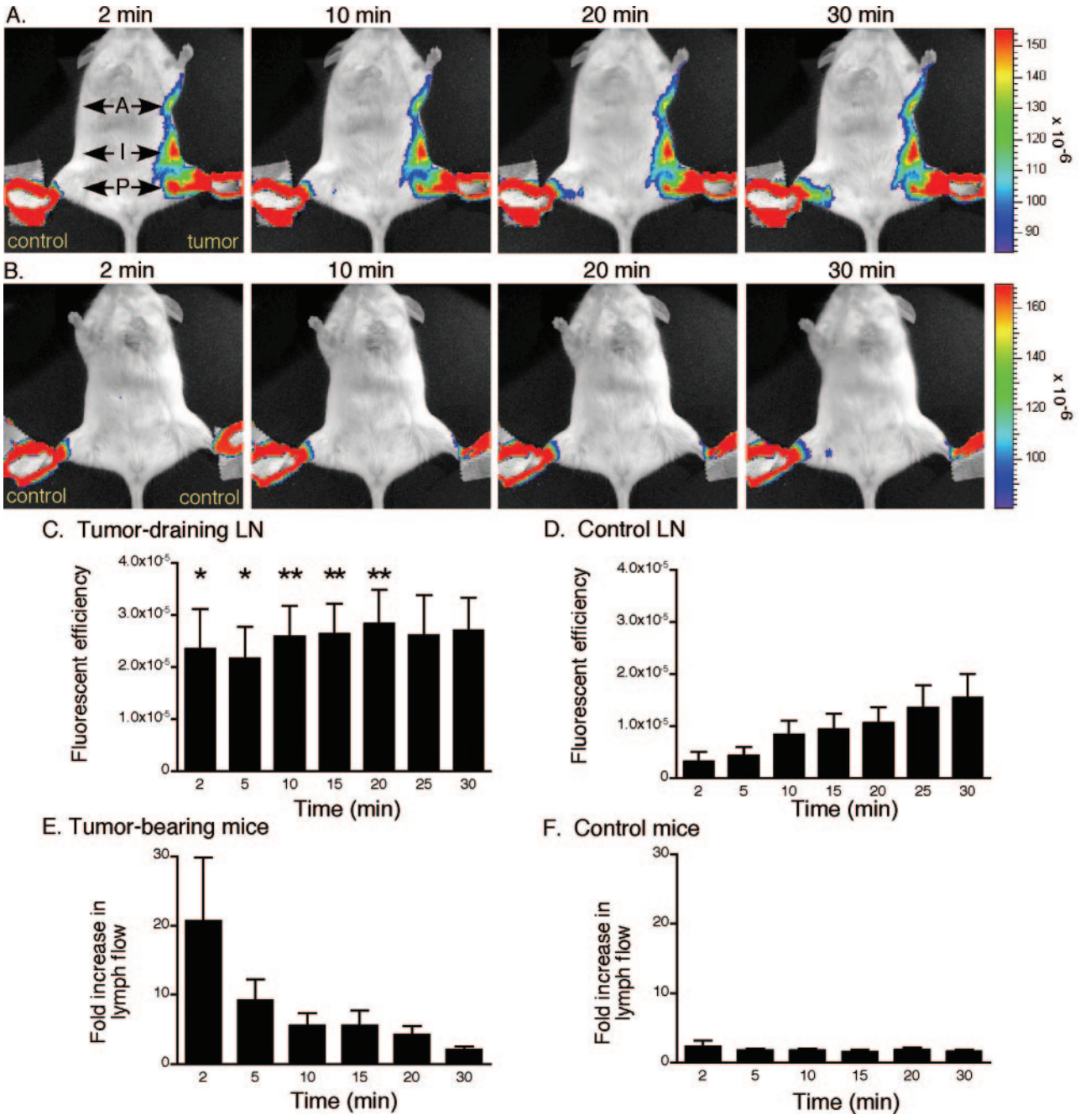

Figure 4. Lymph flow increases in the tumor-draining LNs of albino mice. **A:** Quantum dots were injected into both dorsal rear toes of albino C57Bl/6 mice bearing tumors in the left rear footpad, and mice were imaged from 2 to 30 minutes after injection. Shown is a representative set of supine images. The popliteal LN in the tumor-draining leg (P, **arrow**) is positive for quantum dots within 2 minutes after injection, and the increased signal persists for 30 minutes relative to the control leg. The inguinal (I, **arrow**) and axillary (A, **arrow**) LNs draining the tumor are also positive. **B:** Control albino C57Bl/6 mouse injected with quantum dots shows no visible signal in either popliteal LN until 30 minutes after injection. **C:** Measurement of quantum dot or Cy5.5 nanoparticle fluorescent efficiency in a region of interest drawn over the tumor-draining popliteal LN from eight tumor-bearing mice. Lymph flow is significantly increased in the tumor-draining LN relative to the control nondraining LN by paired *t*-test. $^{*}P < 0.04$, $^{**}P < 0.02$. **D:** Fluorescent efficiency slowly increases in popliteal LN draining the control leg of tumor-bearing mice. **E:** Pairwise comparison of fluorescent efficiency in the tumor-draining and control LNs from individual mice demonstrates increased lymph flow in tumor-draining LNs expressed as a fold increase in lymph flow over the control LNs. **F:** Control mice not bearing tumors showed no difference in lymph flow through each popliteal LN. Standard errors are shown.

black mice showed extensive growth of 10.1.1-positive lymphatic sinuses relative to control nondraining LN (Figure 5A). MECA-32-positive blood vessels were similar in the control and tumor-draining LNs (Figure 5B). Quantification confirmed that lymphatic vessel area increases 12-fold in tumor-draining LNs (Figure 5C), whereas blood vessel density is unaffected (Figure 5D). This specific activation of LN lymphatic vessel growth is very similar to that observed with GFP or melanin antigen-expressing tumors (Figures 2 and 3). These findings indicate that LN lymphangiogenesis is not due to expression of foreign antigens and instead involves a response to tumor growth.

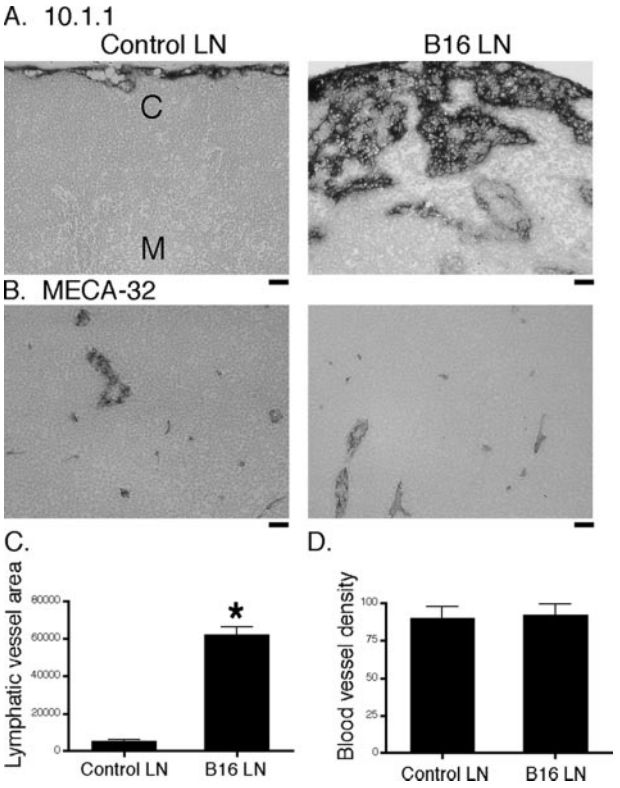

Figure 5. Lymphangiogenesis in LNs draining tumors that do not express foreign antigen. **A:** Popliteal LNs from the control leg of black (melanin-positive) mice implanted with unmarked (GFP-negative) tumors show few cortical (C) or medullary (M) lymphatic sinuses with 10.1.1 immunostaining (left panel), whereas B16 tumor-draining popliteal LN shows extensive growth of lymphatic sinuses throughout the cortex and medulla (right panel). **B:** MECA-32-positive blood vessels are equally abundant in control (left panel) or tumor-draining (right panel) LNs. Scale bars = 25 μm. **C:** Quantification of lymphatic vessel area demonstrates a 12-fold increase in lymphatic vessels in six tumor-draining LNs versus six control LNs, which is statistically significant by *t*-test ($^*P < 0.0001$, $N = 24$). **D:** Blood vessel density is equal in tumor-draining LNs compared with control LNs ($N = 16$). Standard errors are shown.

We adapted the imaging assay to measure lymph flow in black tumor-bearing mice using near infrared quantum dots. The legs were shaved to remove black fur, as it blocks fluorescence detection.[26] Black mice bearing unmodified melanomas in the left rear footpad showed nanoparticles appearing in the tumor-draining popliteal LN within 2 minutes after injection and increasing over 30 minutes, whereas they appeared much more slowly in the control leg LN (data not shown). Quantification of popliteal LN fluorescent signals showed significantly higher levels of lymph flow through the tumor-draining LN from 2 through 30 minutes after injection (Figure 6A), whereas lymph flow slowly increased in the control leg LN (Figure 6B). Comparison of the popliteal LN signal in tumor-draining versus nondraining LNs of individual mice identified a 33-fold increase in quantum dots in the tumor-draining LN relative to the control LN within 2 minutes, and increased lymph flow was sustained over 30 minutes after injection (Figure 6C). This rapid lymph flow profile is very similar to that observed for albino mice bearing GFP-positive tumors (Figure 4). These findings indicate that the increased lymph flow through tumor-draining LNs involves a response to tumor growth, rather than a response to GFP or melanin antigens.

Inflammatory Cells Accumulate in B16 Footpad Tumors and Tumor-Draining LNs

Because the lymphangiogenesis we observe in tumor-draining popliteal LNs occurs in the absence of metastatic B16 tumor cells, we hypothesized that inflammatory cells could traffic from the footpad to the draining LN and produce signals that induce LN-specific lymphangiogenesis. For example, macrophages often infiltrate tumors and can induce lymphatic vessel growth by secreting lymphatic endothelial growth factors such as VEGF-A, VEGF-C, and VEGF-D.[34,35] Moreover, B lymphocytes can strongly promote lymphangiogenesis, in part by secreting VEGF-A.[18,36] Thus, we used immunostaining to assess infiltration of macrophages and B lymphocytes in the primary tumor and draining LN from black C57Bl/6 mice implanted with unmarked B16-F10 cells. The F4/80

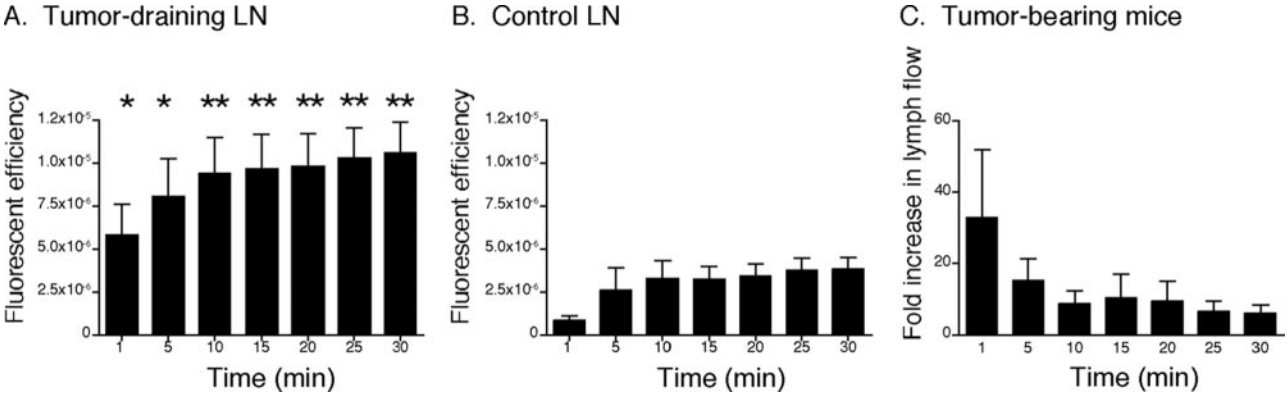

Figure 6. Lymph flow increases in the tumor-draining LN of black mice. Black C57/Bl6 mice implanted with unmarked B16 tumors were imaged after quantum dot injection into both rear dorsal toes, and quantum dot fluorescent efficiency was measured in regions of interest over the popliteal LN in the tumor-draining and control legs from 10 tumor-bearing mice. Quantum dot accumulation is increased in the B16 tumor-draining popliteal LN (**A**) relative to the nondraining control leg LN (**B**) from 2 through 30 minutes of imaging, and this difference is statistically significant ($^*P < 0.04$, $^{**}P < 0.03$). Pairwise comparison of lymph flow through the tumor-draining versus control LNs from individual mice (**C**) demonstrates increased lymph flow through the tumor-draining LNs. Standard errors are shown.

and Mac-1 antibodies were used to detect antigens expressed on macrophages as well as some types of leukocytes.[37,38] The primary footpad tumors showed dense accumulations of Alexa 568-labeled F4/80- and/or FITC-labeled Mac-1-positive cells (Figure 7B, right panel), whereas positive cells were rarely detected in the control footpad (Figure 7B, left panel). Many cells were positive for both the macrophage markers F4/80 and Mac-1. The cells that are positive for only F4/80 or Mac-1 could be granulocytes[37] or eosinophils,[38] respectively. These findings indicate that there is extensive infiltration of macrophages and other leukocytes within the primary footpad tumor, which could potentially contribute to signaling of lymphangiogenesis within the tumor-draining LN.

The LNs were then examined to test whether the macrophage or leukocyte content of the tumor-draining LN is also increased. Alexa 568-labeled F4/80 or FITC-labeled Mac-1-positive cells were rarely observed in the control popliteal LN (Figure 7E, left panel) or in the tumor-draining LN (Figure 7E, right panel). These findings indicate that whereas myeloid cells infiltrate the primary tumor, they do not accumulate within the tumor-draining LN.

A recent study indicated that immunization with bacterial antigens induces inflammation at the injection site, accompanied by accumulation of B lymphocytes and lymphangiogenesis in the draining LN.[36] To determine whether B cells may be present in B16 tumors, we performed immunostaining using the B cell-specific B220 antibody. Footpad tumors or control footpads did not contain FITC-labeled B220-positive B lymphocytes (Figure 7C), indicating that macrophage infiltration of the primary tumor does not involve B lymphocytes. Control LNs showed a normal distribution of FITC-labeled B220-positive B cells confined to the cortical region adjacent to cortical Alexa 568-labeled 10.1.1-positive lymphatic sinuses (Figure 7F, left panel). In contrast, B cells were found throughout the enlarged tumor-draining LN, among the expanded lymphatic sinuses of the cortex and medulla (Figure 7F, right panel). Flow cytometry analysis of B220-positive B lymphocytes and CD3-positive T cells identified a significant eightfold increase in B cell content within tumor-draining LNs relative to the control LNs, in addition to a threefold increase in CD3-positive T cell content (Figure 8). These findings indicate that B and T lymphocytes accumulate in the tumor-draining LN but not in the primary tumor.

B Lymphocytes Are Required for Tumor-Draining LN Lymphangiogenesis

The major alteration we identified thus far, which correlates with tumor-draining LN lymphangiogenesis, is the accumulation of B lymphocytes and, to a lesser extent, T lymphocytes in the draining LN. We next directly examined a role for B lymphocytes in B16 tumor-associated LN lymphangiogenesis using homozygous μMT transgenic mice, which are deficient for B lymphocytes due to deletion of the membrane segment of the Igμ heavy chain gene.[39] B16 tumor cells were injected into the footpad of μMT mice, where they grew at the same rate as tumors transplanted into wild-type mice, reaching 3 to 6 mm diameter within 18 to 22 days (data not shown). Immunostaining for the Alexa 568-labeled 10.1.1 lymphatic endothelial marker demonstrated that the tumor-draining LN does not undergo lymphangiogenesis in μMT mice deficient for B lymphocytes (Figure 7G, right panel). Furthermore, additional immunostaining revealed that F4/80- and Mac-1-positive cells accumulated in the footpad tumors of μMT mice (Figure 7D, right panel) to the same extent as in wild-type mice (Figure 7B, right panel). These findings indicate that macrophage infiltration of the footpad tumor is not sufficient to induce LN lymphangiogenesis. Instead, B lymphocyte accumulation within the draining LN is required for the expansion of LN lymphatic sinuses in response to tumor growth.

LN Lymphangiogenesis Is Required for Tumor-Induced Lymph Flow

Our finding that μMT mice do not undergo lymphangiogenesis in the tumor-draining LN allowed us to test whether this LN lymphangiogenesis is required to increase lymph flow from tumors. The Xenogen lymph flow assay was used to compare lymph flow through the popliteal LN in the tumor-draining and control leg of μMT mice. As previously shown, wild-type mice implanted with B16 footpad tumors exhibited a 33-fold increase in lymph flow by 2 minutes after injection, which persisted over 30 minutes at much higher levels than normal (Figure 6). In μMT mice, lymph flow through the tumor-draining popliteal LN was increased only threefold relative to the control LN, by 2 minutes after quantum dot injection, decreasing to twofold over normal by 10 minutes after injection (Figure 9, black bars). The differences between lymph flow in μMT and wild-type mice were statistically significant from the 5 to 30 minute time points (Figure 9). These findings demonstrate that B cell-associated LN lymphangiogenesis is required to increase lymph flow through the tumor-draining LN.

Discussion

Increasing evidence supports involvement of the lymphatic system in metastasis of a variety of cancers, although little is known yet about the mechanism of tumor cell dissemination. In this study, we found that B16 melanomas, which are thought to metastasize via the lymphatics, surprisingly do not show lymphatic vessel growth in or adjacent to footpad tumors. In fact, tumor lymphatic vessels seemed normal even after tumors metastasized to the draining LN. Instead, we discovered that the popliteal LNs draining the footpad tumors undergo early and extensive growth of lymphatic sinuses, even before tumor cells are detectible within the LNs. These findings demonstrate that tumor-derived signals promote lymphangiogenesis in the draining LN at a distance. We also found that tumor-derived lymphangiogenesis is restricted to the tumor-draining LN, since popliteal LNs from the control rear leg or from the internal mesenteric

LN show normal sparse lymphatics. These results suggest that tumor-derived signals are transported via the lymphatics to the draining LN, where they induce localized lymphatic vessel growth. Lymphangiogenesis has also been identified in the LNs of mice developing lymphomas[18] and in LNs draining murine squamous cell carcinomas.[40] Human LNs infiltrated with metastatic melanoma[13] also show lymphatic vessel growth, suggesting that sentinel LN lymphangiogenesis may be a common feature of murine and human cancers, which could contribute to tumor dissemination.

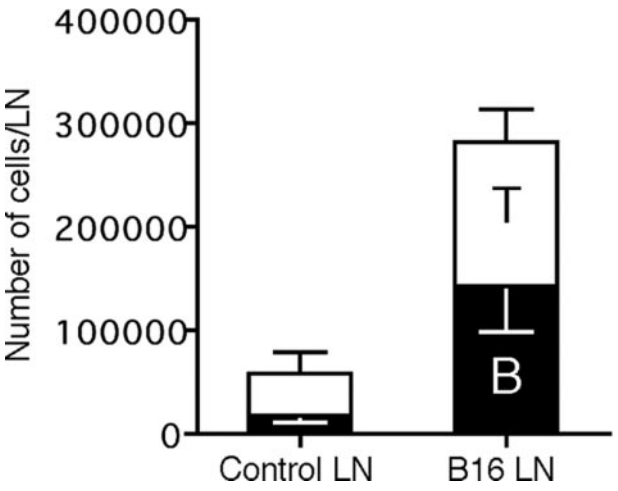

Figure 8. Lymphocytes accumulate in tumor-draining LNs. B220-positive B lymphocytes (black bar) and CD3-positive T lymphocytes (white bar) from control or B16 LNs were measured by flow cytometry. B cell content was significantly increased in tumor-draining LNs, and this change was statistically significant by *t*-test ($N = 3$, $P < 0.05$).

The extensive lymphangiogenesis we identified in B16 melanoma-draining LN is associated with a 20- to 30-fold increase in lymph flow from the dorsal toe through the tumor-draining LN. A previous study observed a two- to sixfold increase in radiotracer clearance out of B16 footpad tumors,[41] supporting our finding that lymph flow is increased from the foot on through the draining LN. Lymphatic vessels are thought to propel lymph by passive influx of fluid into initial lymphatics because of higher tissue interstitial fluid pressure and by spontaneous contraction of smooth muscle cells enveloping the collecting lymphatic vessels.[42,43] Tumors often increase interstitial fluid pressure,[11,44] which could contribute to the ob-

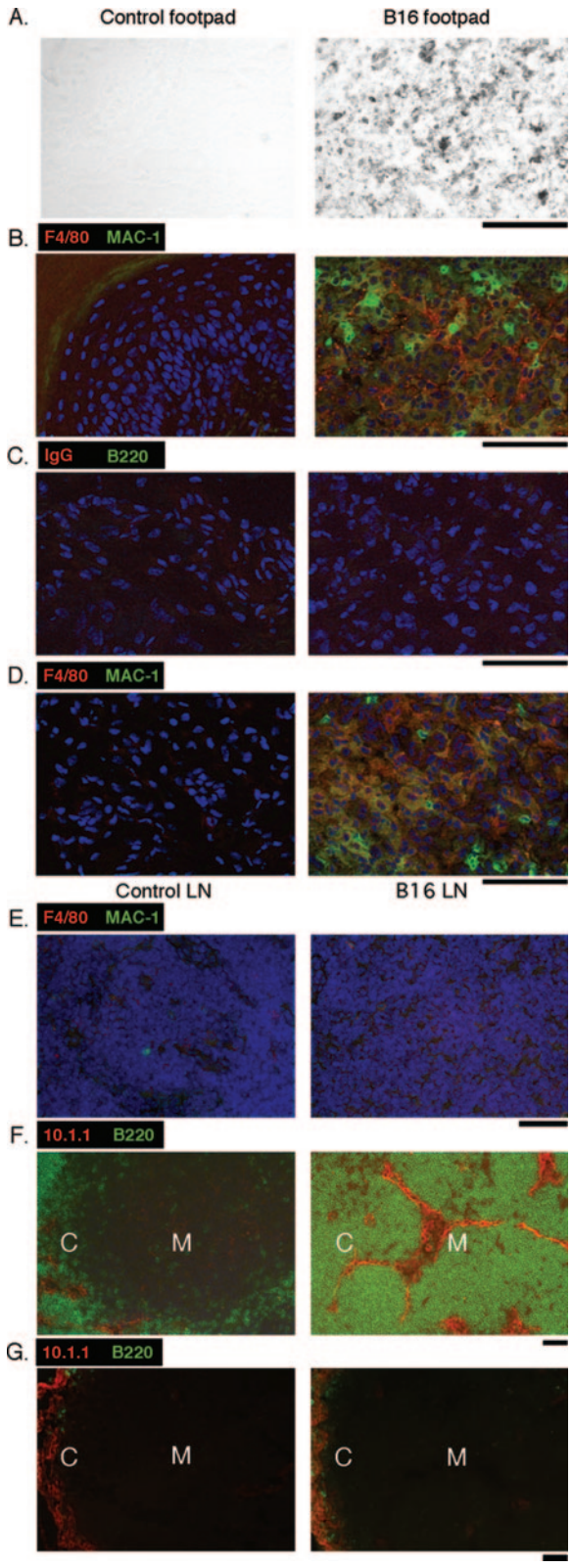

Figure 7. Immune cell accumulation in the primary tumor and tumor-draining LN. **A:** Light microscopy of control (left panel) or B16-implanted (right panel) footpads identifies black-pigmented melanoma cells restricted to the B16 footpad. **B:** Immunostaining of the same footpad regions with Alexa 568-labeled F4/80 and FITC-labeled Mac-1 antibodies shows extensive accumulation of F4/80 and/or Mac-1-positive macrophages and other leukocytes throughout the footpad tumor (right panel) in wild-type mice, whereas these cells were absent from the control footpad (left panel). Nuclei are stained with DAPI. **C:** FITC-labeled B220 immunostaining shows that there are no B lymphocytes in control or B16 footpads of wild-type mice. Control Alexa 568-labeled anti-rat IgG antibodies show no immunostaining of footpads. **D:** Alexa 568-labeled F4/80 and FITC-labeled Mac-1-positive cells are abundant in footpad tumors (right panel) but not in control footpads (left panel) from μMT B cell-deficient mice. **E:** Control (left panel) or tumor-draining (right panel) LNs from wild-type mice show few Alexa 568-labeled F4/80 or FITC-labeled Mac-1-positive cells. **F:** FITC-labeled B220-positive lymphocytes and Alexa 568-labeled 10.1.1-positive lymphatic sinuses are restricted to the cortex (C) of control LN (left panel), whereas B16 tumor-draining LN features B220-positive B lymphocyte accumulation throughout the cortex and medulla (M) alongside enlarged 10.1.1-positive lymphatic sinuses (right panel). **G:** LN from μMT mice do not contain FITC-labeled B220-positive B lymphocytes, and Alexa 568-labeled 10.1.1-positive lymphatic sinuses are restricted to the cortex of both control (left panel) or tumor-draining (right panel) LNs. Scale bars = 50 μm.

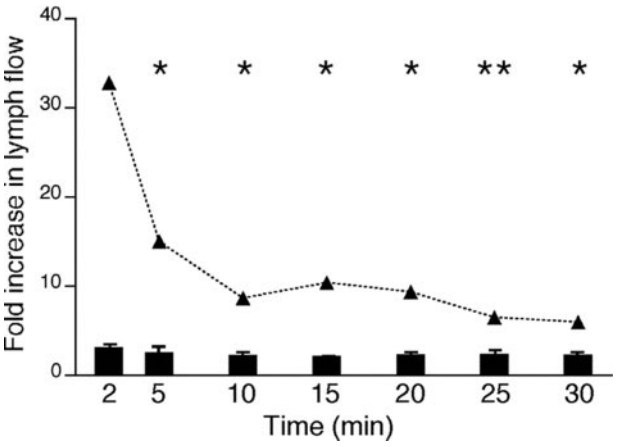

Figure 9. Normal lymph flow through tumor-draining LN in μMT B lymphocyte-deficient mice. Quantum dots were injected into both feet of tumor-bearing μMT mice, and regions of interest were quantitated over 30 minutes of Xenogen imaging in four mice. Lymph flow through the tumor-draining LN was not significantly increased relative to the control leg LN (black bars), in contrast to the large increase in lymph flow through the tumor-draining LNs of wild-type mice (data from Figure 6C shown as a **dashed line**). This difference in lymph flow through the tumor-draining LN of μMT and wild-type mice is statistically significant by *t*-test ($^{*}P < 0.04$, $^{**}P < 0.02$).

served increase in lymph flow. However, we injected the dorsal toe of these mice, which is located several millimeters away from the footpad tumor, so that fluid pressure would need to increase over some distance from the tumor to influence toe lymphatic function.

Although the lymphatic vessels draining the toe and footpad seem normal, a previous study identified a 20 to 60% increase in the diameter of the major lymphatic vessel emptying into the popliteal LN draining B16 footpad tumors,[41] which could promote tumor-draining lymph flow. However, in this study we found that tumor-derived signals exert a much more pronounced effect on lymphatic sinuses within the draining LNs of wild-type mice, as the lymphatic sinus area is increased more than ninefold, and the ellipsoid volume[45] of the popliteal LN is four times larger than normal (data not shown). Taken together, these findings indicate that the major alteration associated with increased lymph flow in wild-type mice is the extensive growth of LN lymphatic sinuses. Moreover, we show in this study that tumor-draining LNs of μMT B cell-deficient mice show normal low lymph flow, which is associated with a failure to induce LN lymphangiogenesis in the tumor-draining LN. These findings suggest that LN lymphangiogenesis actively promotes lymph drainage from the tumor. This hypothesis is supported by our previous finding that lymph flow is greatly increased in Eμ-*c-myc* transgenic mice developing lymphomas, where lymphangiogenesis is restricted to LNs.[18] Further investigation should identify the mechanism of increased lymph flow associated with LN lymphangiogenesis.

Macrophages and other leukocytes infiltrate B16 footpad tumors, whereas B cells accumulate throughout tumor-draining LNs. A recent study also identified alterations in immune cell trafficking into B16 tumor-draining LN, with decreased homing and sticking of naïve lymphocytes in LN high endothelial venules and modestly increased rolling and sticking of polymorphonuclear cells.[46] Taken together, these studies indicate that immune cell function is significantly altered from primary tumors through tumor-draining LNs. Our studies in B cell-deficient μMT mice further indicate that macrophage infiltration of the footpad tumors is not sufficient to induce LN lymphangiogenesis, since μMT mice show extensive macrophage infiltration of the footpad tumors similar to that of wild-type mice, whereas not exhibiting LN lymphangiogenesis. In contrast, B lymphocyte accumulation in the tumor-draining LN is required for LN lymphangiogenesis and increased lymph flow, as μMT mice lacking B cells did not show these lymph node alterations. The contribution of tumor-infiltrating macrophages to vessel alterations in the draining LN remains to be defined.

B cell accumulation within LNs is also associated with LN lymphangiogenesis in Eμ-*c-myc* mice developing lymphomas.[18] Moreover, a recent study demonstrated that immunization with bacterial antigens results in B cell accumulation in draining LNs, which induces LN lymphangiogenesis.[36] In both models, B cell accumulation was associated with increased VEGF-A production in the LN. Further support for these associations were obtained in a study of transgenic mice expressing high levels of VEGF-A in tumor cells, which induced lymphangiogenesis in the tumor-draining LN.[40] VEGF-A may not be the only factor inducing LN lymphangiogenesis, as inhibition of VEGFR-2 signaling only partially inhibited LN lymphangiogenesis in response to bacterial immunization.[36] Inhibition of VEGFR-3 signaling also partially inhibited LN lymphangiogenesis,[36] indicating that VEGF-C or VEGF-D could also promote expansion of LN lymphatic sinuses. We were unable to detect VEGF-A or VEGF-C within the B16 tumor-draining LN by immunostaining (data not shown). However, these factors activate lymphatic endothelial proliferation at very low concentrations,[47,48] so that biologically significant accumulation within tumor-draining LNs may not be detectible. The LN of Eμ-*c-myc* transgenic mice, which are filled with VEGF-A-producing immature B cells, show extensive growth of blood as well as lymphatic vessels,[18] whereas in this study we find that B16 tumor-draining LNs show lymphatic but not blood vessel growth. This suggests that multiple factors regulate blood versus lymphatic vessel growth within the LN. Further analysis of B cell-derived signals should give insight to the contributions of VEGF-A and other growth factors to lymphatic vessel growth in tumor-draining LNs.

Although the tumor-draining lymph nodes undergo extensive lymphangiogenesis, the primary B16 melanomas showed no sign of lymphatic or blood vessel growth. B16-F10 melanomas are known to produce VEGF-A, and the tumor-infiltrating macrophages could potentially contribute VEGF-A, VEGF-C, and VEGF-D,[35] which should promote blood as well as lymphatic vessel growth.[49] Our failure to identify vessel growth in B16 melanomas suggests that additional factors regulate the activity of endothelial growth factors within the primary tumor.

The recruitment of macrophages to B16 tumors and the associated B lymphocyte accumulation in draining LNs is surprising in light of multiple reports that the B16 melanoma is poorly immunogenic in syngeneic mice, allowing tumors to readily grow and metastasize after

implantation,[50] whether or not foreign antigens are expressed from the tumor.[51,52] It remains to be determined why B16 tumors fail to produce an effective anti-tumor immune response. Immune cell infiltration is often associated with immunological tolerance to tumors, in part by VEGF-A-mediated inhibition of dendritic cell function.[53] A similar mechanism could operate in B16 melanomas, which secrete high levels of VEGF-A.[54]

Our finding that B16 tumors induce LN lymphangiogenesis and increase lymph flow through tumor-draining LN suggests that these alterations could actively promote lymphatic metastasis of melanoma cells to draining LN and subsequently to the lungs. Increased lymph propulsion through tumor-draining LNs could reduce fluid pressure within initial lymphatic vessels, promoting tumor cell entry into the occasional lymphatic vessels found in or around the melanomas. After entry into lymphatic vessels, tumor cell transit into and through the draining LNs could be further promoted by increased lymph flow. In support of the idea that LN alterations promote metastasis, we did not observe LN metastasis in μMT B cell-deficient mice showing normal lymph flow. Examination of additional murine and human cancers should determine whether tumor-draining LN lymphangiogenesis and increased lymph flow is a feature of cancers in general or if these alterations are predictive for those cancers that metastasize via the lymphatics. In either case, the development of noninvasive imaging methods to measure LN lymphatic sinuses or lymph flow could provide a useful tool for cancer diagnosis. A requirement for B lymphocytes in stimulating LN alterations, resulting in lymphatic tumor dissemination, could also provide a new target for the development of therapies to block metastasis.

Acknowledgments

We thank Sean Parghi, Momoko Furuya, Mark Tsang, and Leslie Wilson for excellent assistance, and Andrew Farr for generously providing the 10.1.1 and 8.1.1 antibodies. We thank Helene Sage and Paul Neiman for their advice.

References

1. Cao Y: Emerging mechanisms of tumour lymphangiogenesis and lymphatic metastasis. Nat Rev Cancer 2005, 5:735–743
2. He Y, Karpanen T, Alitalo K: Role of lymphangiogenic factors in tumor metastasis. Biochim Biophys Acta 2004, 1654:3–12
3. Stacker S, Baldwin M, Achen M: The role of tumor lymphangiogenesis in metastatic spread. FASEB J 2002, 16:922–934
4. Stacker SA, Caesar C, Baldwin ME, Thornton GE, Williams RA, Prevo R, Jackson DG, Nishikawa S, Kubo H, Achen MG: VEGF-D promotes the metastatic spread of tumor cells via the lymphatics. Nat Med 2001, 7:186–191
5. Skobe M, Hawighorst T, Jackson DG, Prevo R, Janes L, Velasco P, Riccardi L, Alitalo K, Claffey K, Detmar M: Induction of tumor lymphangiogenesis by VEGF-C promotes breast cancer metastasis. Nat Med 2001, 7:192–198
6. Mandriota SJ, Jussila L, Jeltsch M, Compagni A, Baetens D, Prevo R, Banerji S, Huarte J, Montesano R, Jackson DG, Orci L, Alitalo K, Christofori G, Pepper MS: Vascular endothelial growth factor-C-mediated lymphangiogenesis promotes tumour metastasis. EMBO J 2001, 20:672–682
7. He Y, Kozaki K, Karpanen T, Koshikawa K, Yla-Herttuala S, Takahashi T, Alitalo K: Suppression of tumor lymphangiogenesis and lymph node metastasis by blocking vascular endothelial growth factor receptor 3 signaling. J Natl Cancer Inst 2002, 94:819–825
8. He Y, Rajantie I, Pajusola K, Jeltsch M, Holopainen T, Yla-Herttuala S, Harding T, Jooss K, Takahashi T, Alitalo K: Vascular endothelial cell growth factor receptor 3-mediated activation of lymphatic endothelium is crucial for tumor cell entry and spread via lymphatic vessels. Cancer Res 2005, 65:4739–4746
9. Turner RR, Ollila DW, Krasne DL, Giuliano AE: Histopathologic validation of the sentinel lymph node hypothesis for breast carcinoma. Ann Surg 1997, 226:271–278
10. Morton DL, Hoon DS, Cochran AJ, Turner RR, Essner R, Takeuchi H, Wanek LA, Glass E, Foshag LJ, Hsueh EC, Bilchik AJ, Elashoff D, Elashoff R: Lymphatic mapping and sentinel lymphadenectomy for early-stage melanoma: therapeutic utility and implications of nodal microanatomy and molecular staging for improving the accuracy of detection of nodal micrometastases. Ann Surg 2003, 238:538–549
11. Jain RK: Barriers to drug delivery in solid tumors. Sci Am 1994, 271:58–65
12. Padera TP, Kadambi A, di Tomaso E, Carreira CM, Brown EB, Boucher Y, Choi NC, Mathisen D, Wain J, Mark EJ, Munn LL, Jain RK: Lymphatic metastasis in the absence of functional intratumor lymphatics. Science 2002, 296:1883–1886
13. Dadras S, Lange-Aschenfeldt B, Velasco P, Nguyen L, Vora A, Muzikansky A, Jahnke K, Hauschild A, Hirakawa S, Mihm MC, Detmar M: Tumor lymphangiogenesis predicts melanoma metastasis to sentinel lymph nodes. Mod Pathol 2005, 18:1232–1242
14. Maula SM, Luukkaa M, Granman R, Jackson D, Jalkanen S, Ristamaki R: Intratumoral lymphatics are essential for the metastatic spread and prognosis in squamous cell carcinomas of the head and neck region. Cancer Res 2003, 63:1920–1926
15. Choi WW, Lewis MM, Lawson D, Yin-Goen Q, Birdsong GG, Cotsonis GA, Cohen C, Young AN: Angiogenic and lymphangiogenic microvessel density in breast carcinoma: correlation with clinicopathologic parameters and VEGF-family gene expression. Mod Pathol 2005, 18:143–152
16. Bjorndahl MA, Cao R, Burton JB, Brakenhielm E, Religa P, Galter D, Wu L, Cao Y: Vascular endothelial growth factor-A promotes peritumoral lymphangiogenesis and lymphatic metastasis. Cancer Res 2005, 65:9261–9268.
17. Wong SY, Haack H, Crowley D, Barry M, Bronson RT, Hynes RO: Tumor-secreted vascular endothelial growth factor-C is necessary for prostate cancer lymphangiogenesis, but lymphangiogenesis is unnecessary for lymph node metastasis. Cancer Res 2005, 65:9789–9798
18. Ruddell A, Mezquita P, Brandvold KA, Farr A, Iritani BM: B lymphocyte-specific c-Myc expression stimulates early and functional expansion of the vasculature and lymphatics during lymphomagenesis. Am J Pathol 2003, 163:2233–2245
19. Harris AW, Pinkert CA, Crawford M, Langdon WY, Brinster RL, Adams JM: The Em-c-myc transgenic mouse: a model for high-incidence spontaneous lymphoma and leukemia of early B cells. J Exp Med 1988, 167:353–371
20. Fidler IJ: Selection of successive tumor lines for metastasis. Nat New Biol 1973, 242:148–149
21. Giavazzi R, Garofalo A: B16 melanoma metastasis. Methods in Molecular Medicine. Edited by SA Brooks, U Schumacher. Totowa, NJ, Humana Press, Inc., 2001, pp 223–229
22. Pear W, Nolan G, Scott M, Baltimore D: Production of high-titer helper-free retroviruses by transient transfection. Proc Natl Acad Sci USA 1993, 90:8392–8396
23. Miller AD, Miller DG, Garcia JV, Lynch CM: Use of retroviral vectors for gene transfer and expression. Methods Enzymol 1993, 217:580–599
24. Farr A, Nelson A, Hosier S, Kim A: A novel cytokine-responsive cell surface glycoprotein defines a subset of medullary thymic epithelium in situ. J Immunol 1993, 150:1160–1171
25. Schacht V, Ramirez MI, Hong YK, Hirakawa S, Feng D, Harvey N, Williams M, Dvorak AM, Dvorak HF, Oliver G, Detmar M: T1 alpha/podoplanin deficiency disrupts normal lymphatic vasculature formation and causes lymphedema. EMBO J 2003, 22:3546–3556
26. Troy T, Jekic-McMullen D, Sambucetti L, Rice AB: Quantitative comparison of the sensitivity of detection of fluorescent and bioluminescent reporters in animal models. Mol Imaging 2004, 3:9–23

27. Tilney NL: Patterns of lymphatic drainage in the adult laboratory rat. J Anat 1971, 109:369–383
28. Prevo R, Banerji S, Ferguson DJ, Clasper S, Jackson DG: Mouse LYVE-1 is an endocytic receptor for hyaluronan in lymphatic endothelium. J Biol Chem 2001, 276:19420–19430
29. Leppink DM, Bishopp DK, Sedmak DD, Henry ML, Ferguson RM, Streeter PR, Butcher EC, Orosz CG: Inducible expression of an endothelial cell antigen on murine myocardial vasculature in association with interstitial cellular infiltration. Transplantation 1989, 48:874–877
30. Schacht V, Dadras SS, Johnson LA, Jackson DG, Hong YK, Detmar M: Up-regulation of the lymphatic marker podoplanin, a mucin-type transmembrane glycoprotein, in human squamous cell carcinomas and germ cell tumors. Am J Pathol 2005, 166:913–921
31. Ajiro K, Yoda K, Utsumi K, Nishikawa Y: Alteration of cell cycle-dependent histone phosphorylations by okadaic acid. J Biol Chem 1996, 271:13197–13201
32. Brandvold KA, Ewert DL, Kent SC, Neiman P, Ruddell A: Blocked B cell differentiation and emigration support the early growth of Myc-induced lymphomas. Oncogene 2001, 20:3226–3234
33. Swartz MA: The physiology of the lymphatic system. Adv Drug Deliv Rev 2001, 50:3–20
34. Barbera-Guillem E, Nyhus JK, Wolford CC, Friece CR, Sampsel JW: Vascular endothelial growth factor secretion by tumor-infiltrating macrophages essentially supports tumor angiogenesis, and IgG immune complexes potentiate the process. Cancer Res 2002, 62:7042–7049
35. Schoppmann SF, Birner P, Stockl J, Kalt R, Ullrich R, Caucig C, Kriehuber E, Nagy K, Alitalo K, Kerjaschki D: Tumor-associated macrophages express lymphatic endothelial growth factors and are related to peritumoral lymphangiogenesis. Am J Pathol 2002, 161:947–956
36. Angeli V, Ginhoux F, Llodra J, Quemeneur L, Frenette PS, Skobe M, Jessburger R, Merad M, Randolph GJ: B cell-driven lymphangiogenesis in inflamed lymph nodes enhances dendritic cell mobilization. Immunity 2006, 24:203–215
37. Ho MK, Springer TA: Mac-1 antigen: quantitative expression in macrophage populations and tissues, and immunofluorescent localization in spleen. J Immunol 1982, 128:2281–2286
38. McGarry MP, Stewart CC: Murine eosinophil granulocytes bind the murine macrophage-monocyte specific monoclonal antibody F4/80. J Leukoc Biol 1991, 50:471–478
39. Kitamura D, Roes J, Kuhn R, Rajewsky K: A B cell-deficient mouse by targeted disruption of the membrane exon of the immunoglobulin mu chain gene. Nature 1991, 350:423–426
40. Hirakawa S, Kodama S, Kunstfeld R, Kajiya K, Brown LF, Detmar M: VEGF-A induces tumor and sentinel lymph node lymphangiogenesis and promotes lymphatic metastasis. J Exp Med 2005, 201:1089–1099
41. Nathanson SD, Avery M, Anaya P, Sarantou T, Hetzel FW: Lymphatic diameters and radionuclide clearance in a murine melanoma model. Arch Surg 1997, 132:311–315
42. von der Weid PY, Zawieja DC: Lymphatic smooth muscle: the motor unit of lymph drainage. Int J Biochem Cell Biol 2004, 36:1147–1153
43. Ohhashi T, Mizuno R, Ikomi F, Kawai Y: Current topics of physiology and pharmacology in the lymphatic system. Pharmacol Ther 2005, 105:165–188
44. Hagendoorn J, Tong R, Fukumura D, Lin Q, Lobo J, Padera TP, Xu L, Kucherlapati R, Jain RK: Onset of abnormal blood and lymphatic vessel function and interstitial hypertension in early stages of carcinogenesis. Cancer Res 2006, 66:3360–3364
45. Tomayko MM, Reynolds CP: Determination of subcutaneous tumor size in athymic (nude) mice. Cancer Chemother Pharmacol 1989, 24:148–154
46. Carrière V, Colisson R, Jiguet-Jiglaire C, Bellard E, Bouche G, Al Saati T, Amalric F, Girard JP, M'Rini C: Cancer cells regulate lymphocyte recruitment and leukocyte-endothelium interactions in the tumor-draining lymph node. Cancer Res 2005, 65:11639–11648
47. Keyt BA, Berleau LT, Nguyen HV, Chen H, Heinsohn H, Vandlen R, Ferrara N: The carboxyl-terminal domain (111–165) of vascular endothelial growth factor is critical for its mitogenic potency. J Biol Chem 1996, 271:7788–7795
48. Joukov V, Pajusola K, Kaipainen A, Chilov D, Lahtinen I, Kukk E, Saksela O, Kalkkinen N, Alitalo K: A novel vascular endothelial growth factor, VEGF-C, is a ligand for the Flt4 (VEGFR-3) and KDR (VEGFR-2) receptor tyrosine kinases. EMBO J 1996, 15:290–298
49. Nagy JA, Vasile E, Feng D, Sundberg C, Brown LF, Detmar MJ, Lawitts JA, Benjamin L, Tan X:, Manseau EJ, Dvorak AM, Dvorak HF: Vascular permeability factor/vascular endothelial growth factor induces lymphangiogenesis as well as angiogenesis. J Exp Med 2002, 196:1497–1506
50. Overwijk WW, Restifo NP: B16 as a mouse model for human melanoma. Current Protocols in Immunology. Hoboken, NJ, John Wiley & Sons, Inc, 2000, pp 20.21–20.29
51. Brown DM, Fisher TL, Wei C, Frelinger JG, Lord EM: Tumours can act as adjuvants for humoral immunity. Immunology 2001, 102:486–497
52. Skelton D, Satake N, Kohn DB: The enhanced green fluorescent protein (eGFP) is minimally immunogenic in C57BL/6 mice. Gene Ther 2001, 8:1813–1814
53. Yang L, Carbone DP: Tumor-host immune interactions and dendritic cell dysfunction. Adv Cancer Res 2004, 92:13–27
54. Guba M, von Breitenbuch P, Steinbauer M, Koehl G, Flegel S, Hornung M, Bruns CJ, Zuelke C, Farkas S, Anthuber M, Jauch KW, Geissler EK: Rapamycin inhibits primary and metastatic tumor growth by antiangiogenesis: involvement of vascular endothelial growth factor. Nat Med 2002, 8:128–135